Targeting N-myristoylation through NMT2 prevents cardiac hypertrophy and heart failure

Yusuke Tomita[1], MD, Fumiya Anzai[1], MD, PhD, Tomofumi Misaka[1,2], MD, PhD, Ryo Ogawara[1], MD, Shohei Ichimura[1], MD, Kento Wada[1], MD, PhD, Yusuke Kimishima[1], MD, PhD, Tetsuro Yokokawa[1], MD, PhD, Takafumi Ishida[1], MD, PhD, Yasuchika Takeishi[1], MD, PhD

[1]Department of Cardiovascular Medicine, Fukushima Medical University, Fukushima, Japan. [2]Department of Community Cardiovascular Medicine, Fukushima Medical University, Fukushima, Japan.

Correspondence: Tomofumi Misaka, MD, PhD
Department of Cardiovascular Medicine, Fukushima Medical University
1, Hikarigaoka, Fukushima, 960-1295, Japan
Phone: +81-24-547-1190; Fax: +81-24-548-1821
E-mail: misaka83@fmu.ac.jp

Supplemental Appendix

Supplemental Figures 1-18

Supplemental Tables 1-4

Supplemental Methods

Supplemental References

Data Availability

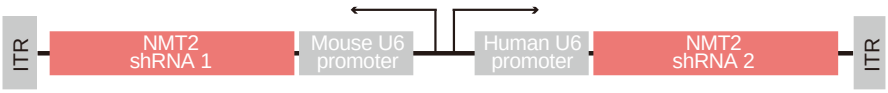

Supplemental Figure 1. Schematic representation of adeno-associated virus 9 (AAV9) vector for knockdown of NMT2 in the hearts.
Two transgenes encoding short hairpin RNA (shRNA) target to mouse NMT2 that are driven by mouse U6 and human U6 promoters with separate loops are packed into a single AAV9 vector. ITR, inverted terminal repeat.

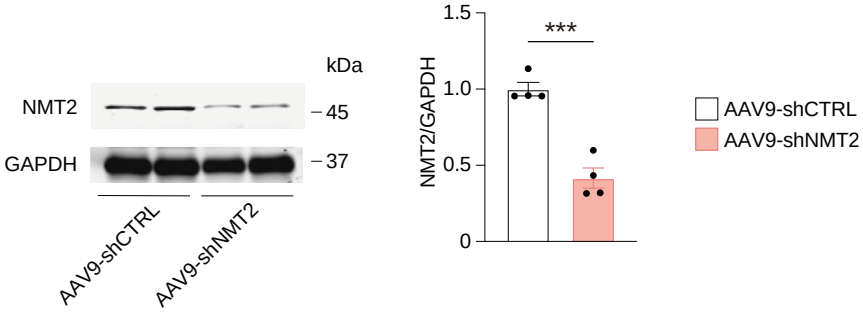

Supplemental Figure 2. Knockdown of cardiac NMT2 by shRNA with AAV9-mediated gene delivery.
Representative immunoblots for cardiac NMT2. The mice at the age of six weeks were injected with 1.0×10^{11} genome-containing units of AAV9 encoding shRNA target to NMT2 (AAV9-shNTM2) or LacZ as a control (AAV9-shCTRL). At three weeks after injections, the protein extracts from the left ventricles were subjected to immunoblotting analysis. GAPDH was used for normalization. Data were expressed over the control. Data are presented as the mean ± SEM (n = 4 in each group). $^{***}P < 0.001$ by the unpaired Student's t-test (two-sided).

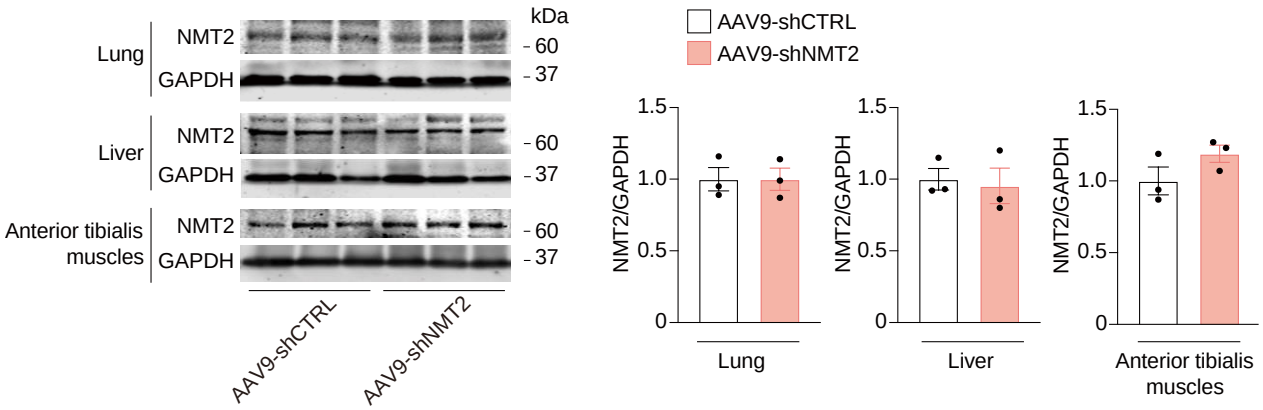

Supplemental Figure 3. NMT2 expressions in the lung, liver, and anterior tibialis muscles after AAV9-shNMT2 injection.
The wild-type mice at the age of six weeks were injected with 1.0×10^{11} genome-containing units of AAV9 encoding shRNA target to NMT2 (AAV9-shNTM2) or LacZ as a control (AAV9-shCTRL). The protein extracts from the lung, liver, and anterior tibialis muscles were subjected to immunoblotting analysis at 3 weeks after AAV9 injections. GAPDH was used for normalization. Data were expressed over the control. Data are presented as the mean ± SEM (n = 3 in each group). Statistical comparison was performed by the unpaired Student's t-test (two-sided).

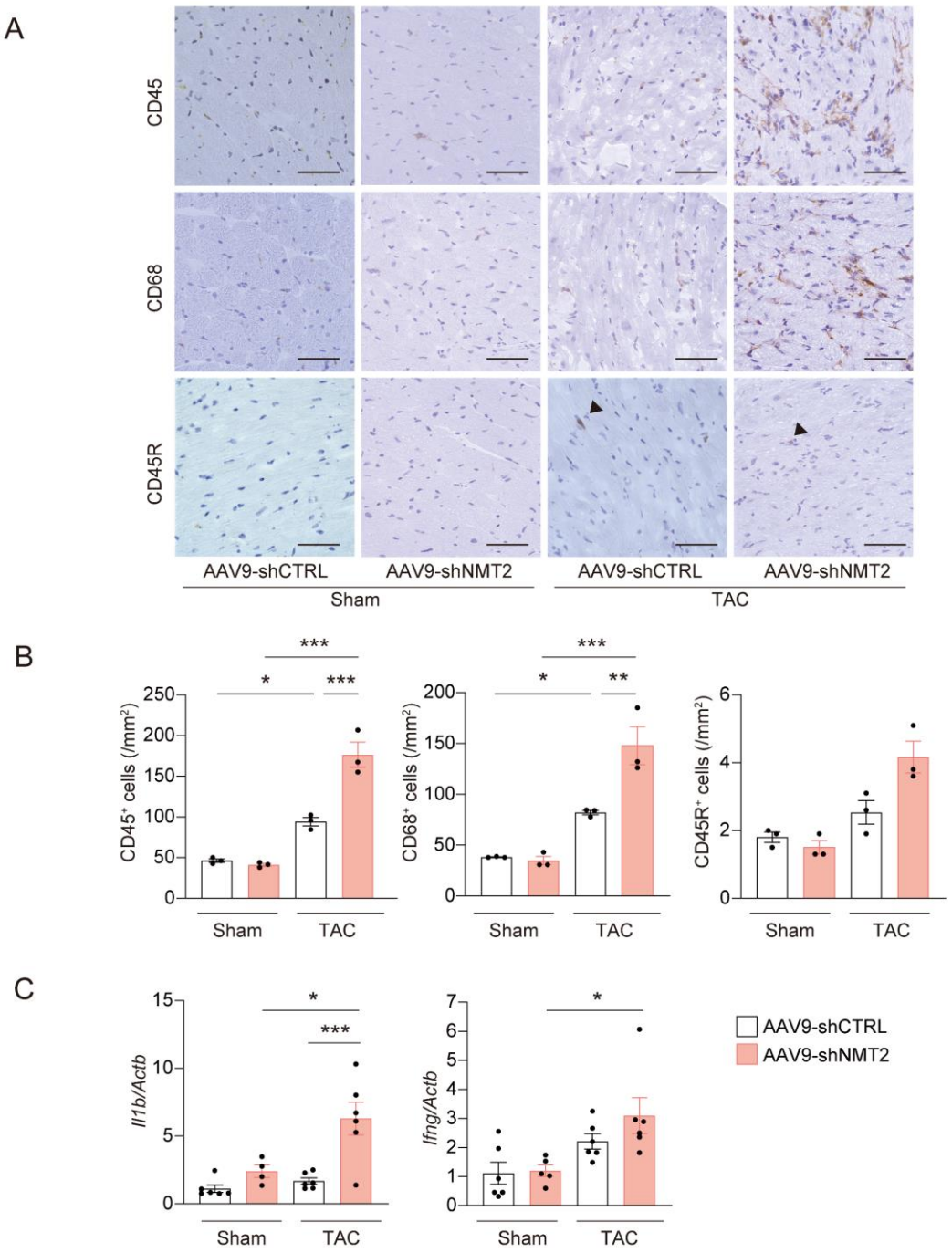

Supplemental Figure 4. Inflammatory cell infiltration in the left ventricles in AAV9-mediated NMT2 knockdown mice after pressure overload.

A, Representative immunohistochemical images in the left ventricles using an anti-CD45 antibody for leukocytes, anti-CD68 for macrophages, and anti-CD45R for B cells in mice receiving either AAV9-shCTRL or AAV9-shNMT2 at 4 weeks after sham or transverse aortic constriction (TAC) operation. Arrow heads indicate CD45R-positive cells. Scale bars, 50 μm. **B**, Quantitative analysis of each infiltrating inflammatory cell type (n = 3 in each group). **C**, Relative mRNA expression levels of *Il1b* and *Ifng* in the hearts. *Actb* was used for normalization (n = 4-6 in each group). The average value for sham-operated AAV9-shCTRL-injected mice was set equal to 1. All data are presented as mean ± SEM. $^{*}P < 0.05$, $^{**}P < 0.01$, and $^{***}P < 0.001$ by one-way ANOVA with Tukey's post hoc analysis.

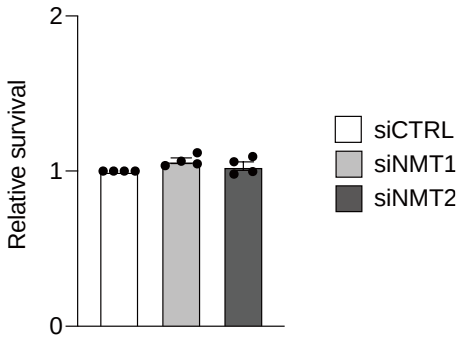

Supplemental Figure 5. Effects of knockdown of NMT1 or NMT2 on cell viability.
H9c2 myocytes were transfected with small interfering RNA specific to NMT1 (siNMT1) or NMT2 (siNMT2). Non-targeting control small interfering RNA (siCTRL) was used as a control. Forty-eight h after transfection, the cell viability was assessed by MTS assay. The value for siCTRL was set equal to 1. Data are presented as the mean ± SEM from 4 independent experiments with triplicates. Statistical comparison was performed by one-way ANOVA.

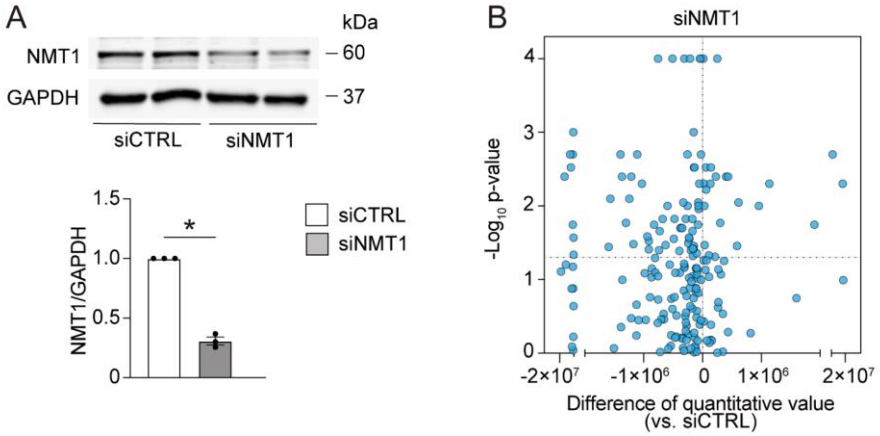

Supplemental Figure 6. Effects of NMT1 knockdown in N-myristoylation as determined through click chemistry-based quantitative proteomics.
A, Western blot analysis of NMT1 in H9c2 myocytes transfected with small interfering RNA specific to NMT1 (siNMT1) or non-targeting control small interfering RNA (siCTRL) for 48 h in H9c2 myocytes. GAPDH served as a loading control. Densitometric analysis is presented in graphs as mean ± SEM (n = 3 in each group). $^{*}P < 0.05$ by the unpaired Student's t-test (two-sided). **B**, Identification of N-myristoylated substrate proteins in cardiac myocytes by click chemistry-based quantitative proteomics in NMT1 knockdown H9c2 cells. Volcano plots for N-myristoylated proteins comparing with siCTRL from three independent experiments performed in triplicate. Statistical comparison was performed by the unpaired Student's t-test (two-sided).

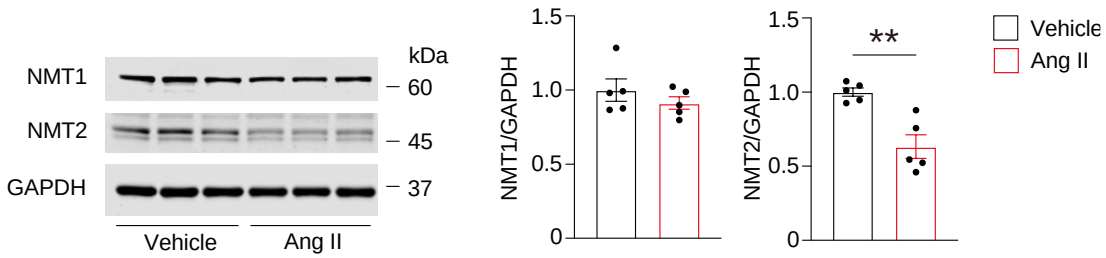

Supplemental Figure 7. NMT2 expression, but not NMT1, was decreased in response to angiotensin II in H9c2 cardiac myocytes.
Immunoblot analysis of NMT1 and NMT2 in protein extracts from H9c2 myocytes treated with angiotensin II (Ang II,1 μM) for 6 h. GAPDH was used as a loading control. Data are expressed over the control, and presented as mean ± SEM (n = 5 in each group). $^{**}P < 0.01$ by the unpaired Student's t-test (two-sided).

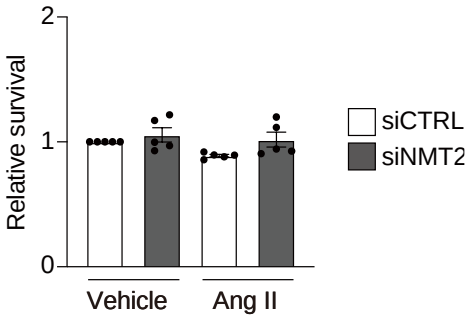

Supplemental Figure 8. Effects of angiotensin II on cell viability on NMT2 knockdown cells.
Transfected H9c2 myocytes with siCTRL or siNMT2 were stimulated with angiotensin II (Ang II, 1 μM) or vehicle for 24 h. The cell viability was assessed by MTS assay. The value for the group with siCTRL and vehicle was set equal to 1. Data are presented as mean ± SEM from 5 independent experiments with triplicates. Statistical comparison was performed by one-way ANOVA.

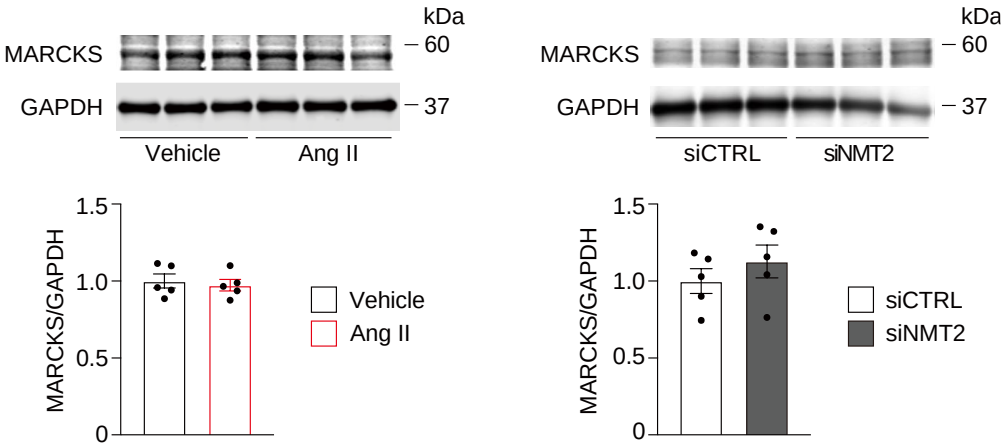

Supplemental Figure 9. No alteration in MARCKS expression in angiotensin II-treated or NMT2 knockdown H9c2 myocytes.
Immunoblot analysis for MARCKS on protein extracts obtained from H9c2 myocytes treated with angiotensin II (Ang II, 1 μM) or vehicle for 24 h (left). The cells were transfected with small interfering RNA specific to NMT2 (siNMT2) or non-targeting control small interfering RNA (siCTRL) for 48 h (right). GAPDH was used for normalization. Data are expressed over the control group and are presented as mean ± SEM (n = 5 in each group). Statistical comparison was performed by the unpaired Student's t-test (two-sided).

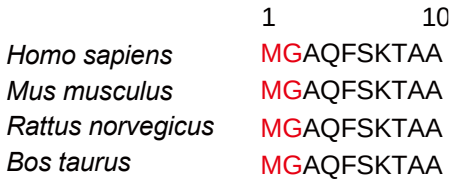

Supplemental Figure 10. Conservation of MARCKS among the species.
N-terminal amino acid residues of MARCKS in *Homo sapiens*, *Mus musculus*, *Rattus norvegicus*, and *Bos taurus* are presented. Numbers are given according to the amino acid sequence from the beginning.

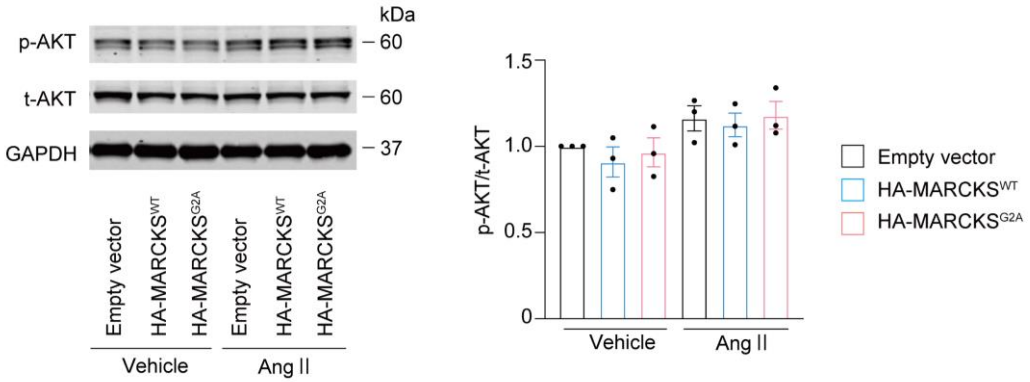

Supplemental Figure 11. Effects of overexpressing MARCKS and mutant MARCKS with G2A on phosphorylation of AKT.
Immunoblot analysis on AKT phosphorylation. H9c2 cells were transfected with hemagglutinin (HA)-tagged wild-type MARCKS (MARCKS^{WT}) or HA-tagged mutant MARCKS with replacement of N-terminal glycine to alanine (MARCKS^{G2A}) for 48 h. An empty vector was used as a negative control. Forty-eight h after transfection, cells were stimulated with angiotensin II (Ang II, 1 μM) or vehicle for 1 h and subjected to immunoblotting. Quantitative analysis of the ratio of phosphorylated AKT (p-AKT) and total AKT (t-AKT) is presented in the graph as mean ± SEM (n = 3 in each group). GAPDH was used as the loading control. The value for the group with an empty vector and vehicle was set equal to 1. Statistical comparison was performed by one-way ANOVA.

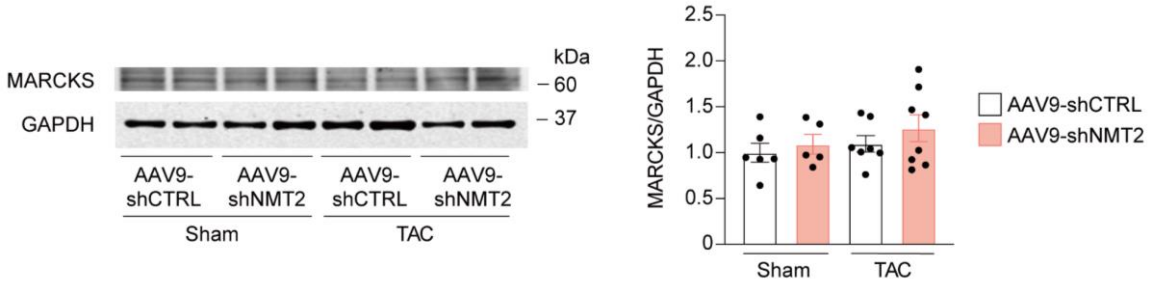

Supplemental Figure 12. MARCKS expression in NMT2 knockdown murine hearts.
Immunoblot analysis for MARCKS in TAC-operated NMT2 knockdown hearts. The protein extracts from the left ventricles in mice receiving either AAV9-shCTRL or AAV9-shNMT2 at four weeks post-sham or -TAC operation were immunoblotted with the indicated antibodies. The ratios of phosphorylated MARCKS to total MARCKS and total MARCKS to GAPDH are quantified and presented in the graphs (n = 5-8 in each group). Statistical comparison was performed by one-way ANOVA.

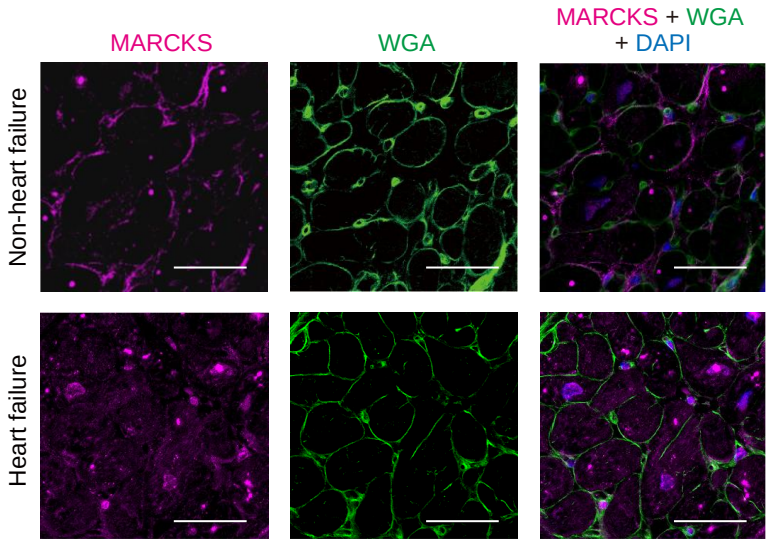

Supplemental Figure 13. Fluorescent immunohistochemical analysis for MARCKS in patients with heart failure.
Triple-labeled immunofluorescent staining (MARCKS, magenta; WGA, green; DAPI, blue) of the heart sections from myocardial biopsy specimens in non-heart failure controls and heart failure patients with dilated cardiomyopathy. Scale bars, 20 μm. Representative images from 6 and 12 individuals in each are shown. WGA, wheat germ agglutinin.

Supplemental Figure 14. Schematic representation of AAV9 vector for overexpression of NMT2 in the hearts. Mouse NMT2 with N-terminal FLAG-tag is packaged into an AAV9 particle. CMV, cytomegalovirus; ITR, inverted terminal repeat.

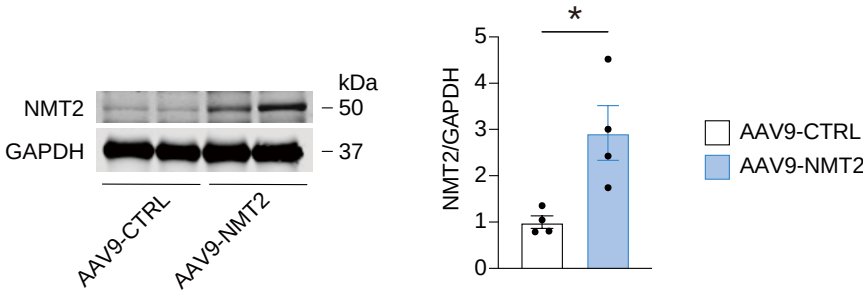

Supplemental Figure 15. Overexpression of cardiac NMT2 by AAV9-mediated gene delivery.
Immunoblots for cardiac NMT2. AAV9 encoding mouse NMT2 with a FLAG-tag (AAV9-NMT2) with 1.0×10^{11} genome-containing units were injected in mice at the age of six weeks. AAV9 encoding mouse LacZ was used as a control (AAV9-CTRL). At three weeks after injections, the protein extracts from the left ventricles were subjected to immunoblotting analysis. GAPDH was used for normalization. Data were expressed over the control. Data are presented as mean ± SEM (n = 4 in each group). $^{*}P < 0.05$ by the unpaired Student's t-test (two-sided).

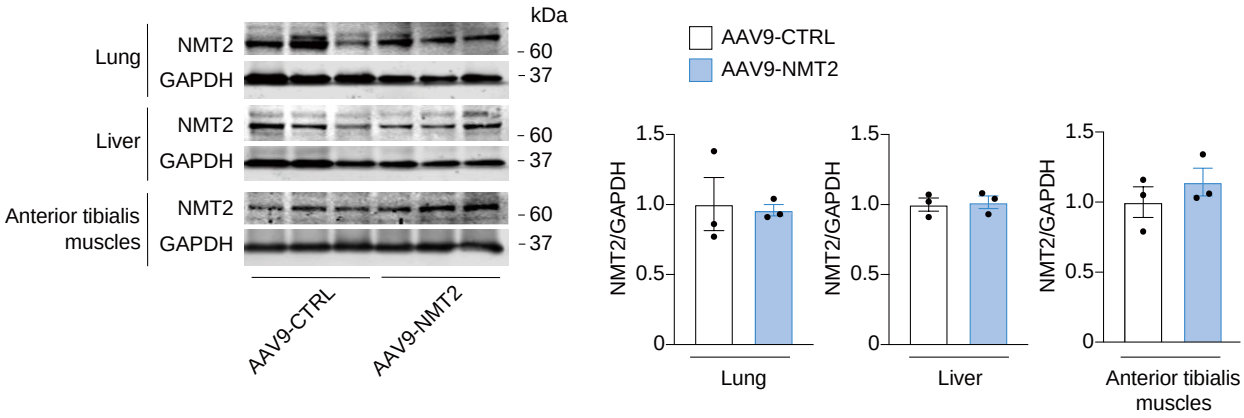

Supplemental Figure 16. NMT2 expression in the lung, liver, and anterior tibialis muscles following injection of AAV9-NMT2.
Six-week-old wild-type mice were injected with either 1.0×10^{11} genome-containing units of AAV9-NMT2 encoding mouse NMT2 with a FLAG-tag, or AAV9-CTRL encoding mouse LacZ as a control. After three weeks, protein extracts from the lung, liver, and anterior tibialis muscles were subjected to immunoblotting analysis, with GAPDH used as the normalization control. The data are presented as mean ± SEM (n = 3 in each group) and expressed relative to the control. Statistical comparison was performed by the unpaired Student's t-test (two-sided).

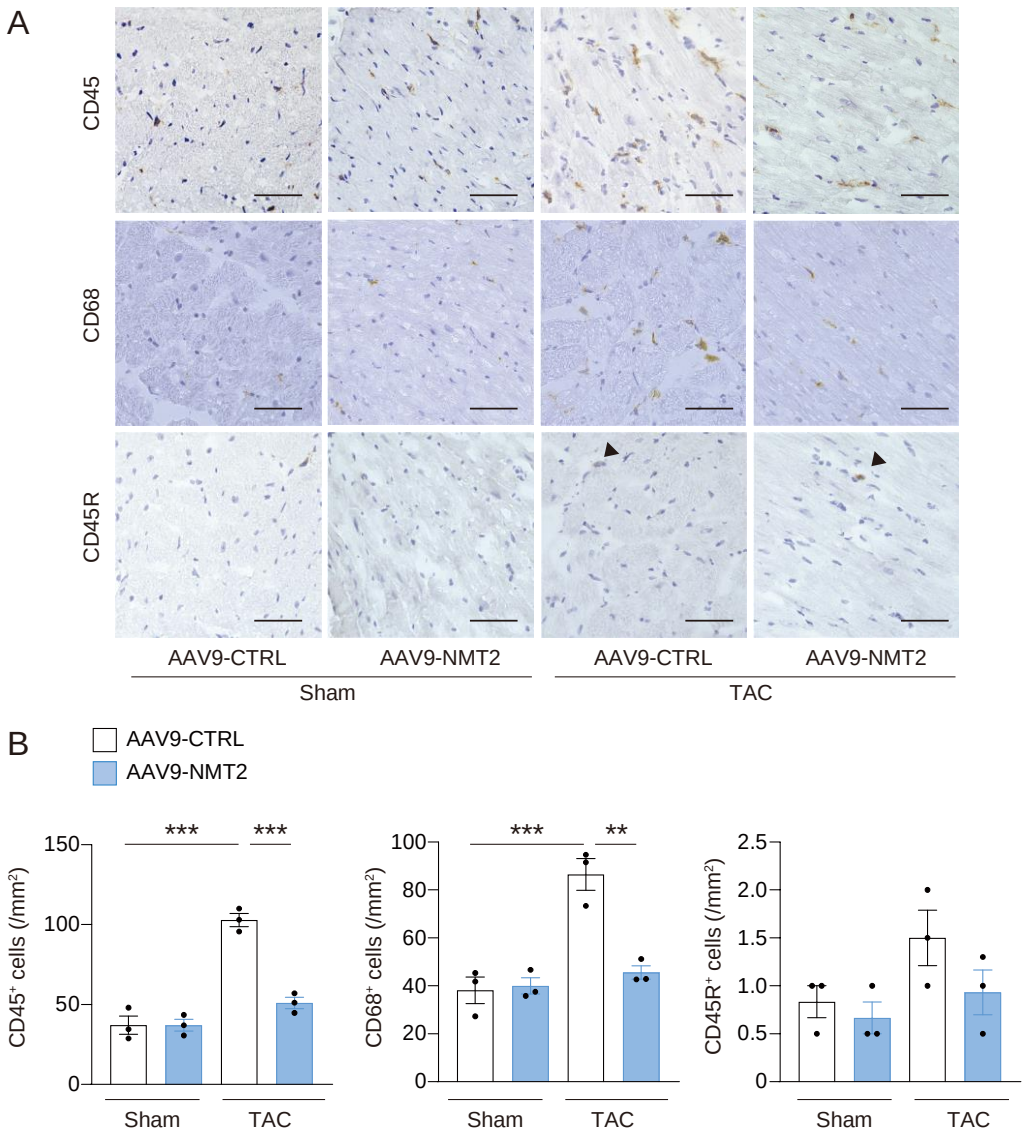

Supplemental Figure 17. Impact of cardiac NMT2 overexpression in immune systems in pressure overload-induced heart failure.

A, Representative immunohistochemical images in the left ventricles using an anti-CD45 antibody for leukocytes, anti-CD68 for macrophages, and anti-CD45R for B cells in mice receiving either AAV9-CTRL or AAV9-NMT2 at 4 weeks after sham or TAC operation. Arrow heads indicate CD45R-positive cells. Scale bars, 50 μm. **B**, Quantitative analysis of each infiltrating inflammatory cell type (n = 3 in each group). All data are presented as mean ± SEM. $^{**}P < 0.01$ and $^{***}P < 0.001$ by one-way ANOVA with Tukey's post hoc analysis.

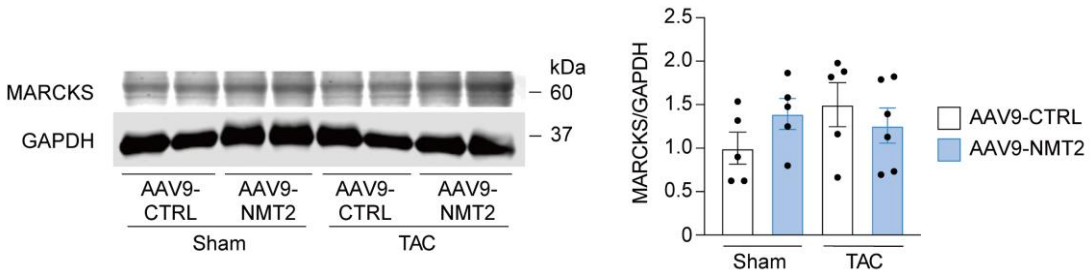

Supplemental Figure 18. MARCKS expression in NMT2-overexpressing murine hearts.

Immunoblot analysis for MARCKS in TAC-operated NMT2 overexpressed mice. The protein extracts from the left ventricles in mice receiving either AAV9-CTRL or AAV9-NMT2 at four weeks post-sham or -TAC operation were immunoblotted with the indicated antibodies. The ratio of MARCKS to GAPDH are quantified and presented in the graphs (n = 5-8 in each group). Statistical comparison was performed by one-way ANOVA.

Supplemental Table 1. Echocardiography in sham- or transverse aortic constriction (TAC)-operated wild-type C57BL/6 mice at 4-week post-surgery.

	Sham (n = 3)	TAC (n = 5)	P value
IVSd, mm	1.11 ± 0.13	1.35 ± 0.12	0.048
LVPWd, mm	1.10 ± 0.11	1.35 ± 0.09	0.022
LV mass, mg	99.8 ± 16.4	189.7 ± 38.2	0.013
LVIDd, mm	2.64 ± 0.02	3.33 ± 0.37	0.024
LVIDs, mm	1.11 ± 0.06	2.39 ± 0.44	0.004
LVFS, %	57.8 ± 2.5	28.4 ± 5.5	<0.001
HR, bpm	634.7 ± 34.6	622.3 ± 48.7	0.72

All data are presented as the mean ± SEM. Pressure overload was induced by constricting the transverse aorta using a 28-gauge blunt needle. IVSd, diastolic interventricular septum wall thickness; LVPWd, diastolic left ventricular posterior wall thickness; LV, left ventricular; LVIDd, end-diastolic left ventricular internal dimension; LVIDs, end-systolic left ventricular internal dimension; LVFS, left ventricular fractional shortening; HR, heart rate.

Supplemental Table 2. Clinical characteristics of patients with idiopathic dilated cardiomyopathy with heart failure and non-heart failure control subjects for immunohistochemical analysis.

	Heart failure (n = 12)	Non-heart failure controls (n = 6)	P value
Age, years	56.3 ± 16.8	53.0 ± 19.5	0.72
Male, n (%)	10 (83.3)	6 (100.0)	0.17
Body mass index, kg/m^2	24.3 ± 3.3	25.3 ± 3.7	0.55
NYHA functional class, III/VI, n (%)	8 (66.7) / 4 (33.3)	N/A	NA
Comorbidity			
Hypertension, n (%)	6 (50.0)	5 (83.3)	0.16
Diabetes mellitus, n (%)	3 (25.0)	1 (16.7)	0.71
Atrial fibrillation, n (%)	5 (41.7)	1 (16.7)	0.28
Chronic kidney disease, n (%)	3 (25.0)	2 (33.3)	0.75
Echocardiography			
Left ventricular ejection fraction, %	27.4 ± 16.4	61.9 ± 9.0	<0.001
Left ventricular end-diastolic dimensions, mm	64.2 ± 5.9	44.0 ± 5.5	0.002
Laboratory data			
B-type natriuretic peptide, pg/mL	300.8 (213.5-464.5)	114.1 (101.9-151.4)	0.001
Troponin I, ng/mL	0.07 (0.06-0.12)	0.03 (0.02-0.04)	0.012
Direct bilirubin, mg/dL	0.11 ± 0.03	0.10 ± 0.00	0.50
Creatinine, mg/dL	0.88 ± 0.15	1.00 ± 0.16	0.16
Estimated GFR, mL/min/1.73m^2	70.0 ± 16.1	66.7 ± 20.5	0.71
C-reactive protein, mg/dL	0.49 (0.24-0.97)	0.09 (0.03-0.17)	0.014
Right heart catheterization			
Cardiac index, L/min/m^2	2.04 ± 0.54	2.91 ± 0.55	0.015
Pulmonary capillary wedge pressure, mmHg	19.4 ± 4.2	12.7 ± 4.5	0.017
Medications			
Beta-blockers, n (%)	10 (83.3)	5 (83.3)	>0.99
Renin-angiotensin system inhibitors, n (%)	11 (91.7)	5 (83.3)	0.62
Mineralocorticoid receptor antagonists, n (%)	8 (66.7)	0 (0)	<0.001
Diuretics, n (%)	7 (58.3)	0 (0)	0.007

Data are presented as the mean ± standard deviation (SD), number (%) or median (25th - 75th percentiles). NA, not applicable; NYHA, New York Heart Association; GFR, glomerular filtration rate. Comparisons of values between the two groups were performed by the unpaired Student's t-test or Mann-Whitney U-test. Categorical variables were compared using Fisher's exact test.

Supplemental Table 3. Echocardiography in AAV9-shCTRL- or AAV9-shNMT2-injected sham- or TAC-operated mice at 1-, 2-, and 4-week.

Parameters at 1-week	AAV9-shCTRL +sham (n = 6)	AAV9-shNMT2 +sham (n = 5)	AAV9-shCTRL +TAC (n = 6)	AAV9-shNMT2 +TAC (n = 12)
IVSd, mm	0.93 ± 0.02	1.13 ± 0.07	1.38 ± 0.07***	1.41 ± 0.06***
LVPWd, mm	1.03 ± 0.04	1.09 ± 0.05	1.42 ± 0.10*	1.50 ± 0.08**
LV mass, mg	81.5 ± 6.1	80.2 ± 5.0	110.6 ± 6.2*	118.0 ± 5.2**
LVIDd, mm	2.60 ± 0.08	2.22 ± 0.14	2.08 ± 0.16	2.11 ± 0.12
LVIDs, mm	1.19 ± 0.06	1.22 ± 0.11	1.11 ± 0.10	1.23 ± 0.05
LVFS, %	54.4 ± 1.6	44.6 ± 5.8	46.0 ± 4.1	39.6 ± 3.9
HR, bpm	667.8 ± 29.9	657.9 ± 11.8	661.6 ± 30.3	614.9 ± 21.4
Peak velocity, m/s	0.7 ± 0.1	0.7 ± 0.1	4.2 ± 0.3***	4.3 ± 0.2***
Peak PG, mmHg	2.3 ± 0.9	2.3 ± 0.7	74.2 ± 10.8***	75.5 ± 5.5***

Parameters at 2-week	AAV9-shCTRL +sham (n = 6)	AAV9-shNMT2 +sham (n = 5)	AAV9-shCTRL +TAC (n = 5)	AAV9-shNMT2 +TAC (n = 8)
IVSd, mm	0.99 ± 0.03	1.06 ± 0.05	1.55 ± 0.11***	1.57 ± 0.07***
LVPWd, mm	0.97 ± 0.04	1.13 ± 0.03	1.66 ± 0.10***	1.68 ± 0.05***
LV mass, mg	75.8 ± 2.8	95.5 ± 8.3	155.2 ± 13.8***	167.2 ± 13.5***
LVIDd, mm	2.50 ± 0.08	2.59 ± 0.10	2.21 ± 0.16	2.30 ± 0.08
LVIDs, mm	1.08 ± 0.09	1.17 ± 0.10	1.30 ± 0.12	1.60 ± 0.09**
LVFS, %	56.9 ± 3.8	55.2 ± 3.2	41.4 ± 1.6**	30.7 ± 2.1***
HR, bpm	673.4 ± 20.7	601.4± 24.3	681.5 ± 29.1	590.3 ± 28.1

Parameters at 4-week	AAV9-shCTRL +sham (n = 6)	AAV9-shNMT2 +sham (n = 5)	AAV9-shCTRL +TAC (n = 5)	AAV9-shNMT2 +TAC (n = 4)
IVSd, mm	1.05 ± 0.04	1.07 ± 0.07	1.53 ± 0.02***	1.45 ± 0.04***
LVPWd, mm	1.17 ± 0.04	1.22 ± 0.07	1.87 ± 0.04***	1.90 ± 0.09***
LV mass, mg	92.5 ± 7.0	97.7 ± 15.2	167.2 ± 17.1**	178.6 ± 4.1***
LVIDd, mm	2.48 ± 0.13	2.45 ± 0.17	2.13 ± 0.16	2.35 ± 0.13
LVIDs, mm	1.13 ± 0.07	1.28 ± 0.10	1.28 ± 0.10	1.72 ± 0.13**†
LVFS, %	54.3 ± 2.0	47.6 ± 1.0	41.7 ± 4.1*	26.5 ± 5.1***†
HR, bpm	695.7 ± 6.7	672.2 ± 12.1	660.6 ± 14.8	659.0 ± 28.3

All data are presented as the mean ± SEM. Pressure overload was induced by constricting the transverse aorta using a 27-gauge blunt needle. $^{*}P < 0.05$, $^{**}P < 0.01$, and $^{***}P < 0.001$ vs. sham-operated AAV9-shCTRL-injected mice. $^{\dagger}P < 0.05$ vs. TAC-operated AAV9-shCTRL-injected mice. Statistical test was performed by one-way ANOVA with Tukey's post hoc analysis. IVSd, end-diastolic interventricular septum wall thickness; LVPWd, end-diastolic left ventricular posterior wall thickness; LV, left ventricular; LVIDd, end-diastolic left ventricular internal dimension; LVIDs, end-systolic left ventricular internal dimension; LVFS, left ventricular fractional shortening; HR, heart rate: PG, pressure gradient.

Supplemental Table 4. Echocardiography in AAV9-CTRL- or AAV9-NMT2-injected sham- or TAC-operated mice at 1-, 2-, and 4-week.

Parameters at 1-week	AAV9-CTRL +sham (n = 7)	AAV9-NMT2 +sham (n = 6)	AAV9-CTRL +TAC (n = 6)	AAV9-NMT2 +TAC (n = 5)
IVSd, mm	1.08 ± 0.06	0.84 ± 0.05	1.02 ± 0.19	1.10 ± 0.09
LVPWd, mm	1.15 ± 0.14	0.98 ± 0.16	0.94 ± 0.21	1.14 ± 0.08
LV mass, mg	78.9 ± 5.3	71.4 ± 12.6	91.1 ± 20.3	103.0 ± 15.5
LVIDd, mm	2.25 ± 0.32	2.53 ± 0.16	2.88 ± 0.29	2.71 ± 0.27
LVIDs, mm	1.24 ± 0.10	1.29 ± 0.24	2.00 ± 0.31	1.48 ± 0.19
LVFS, %	46.3 ± 4.2	53.0 ± 3.3	31.0 ± 3.8***	41.7 ± 1.2
HR, bpm	694.6 ± 43.0	637.3 ± 12.5	617.6 ± 30.0	607.9 ± 11.7
Peak velocity, m/s	1.8 ± 0.6	1.8 ± 0.9	5.6 ± 0.4**	6.1 ± 0.7***
Peak PG, mmHg	18.5 ± 9.9	19.6 ± 16.0	126.3 ± 16.1**	154.1 ± 33.3**

Parameters at 2-week	AAV9-CTRL +sham (n = 7)	AAV9-NMT2 +sham (n = 6)	AAV9-CTRL +TAC (n = 6)	AAV9-NMT2 +TAC (n = 5)
IVSd, mm	0.95 ± 0.07	0.86 ± 0.05	1.23 ± 0.04**	1.05 ± 0.06
LVPWd, mm	0.95 ± 0.09	0.98 ± 0.05	1.32 ± 0.08**	1.22 ± 0.03
LV mass, mg	71.5 ± 6.3	61.1 ± 4.4	143.3 ± 12.6***	94.4 ± 8.5††
LVIDd, mm	2.55 ± 0.12	2.28 ± 0.08	3.03 ± 0.27	2.45 ± 0.14
LVIDs, mm	1.29 ± 0.12	0.97 ± 0.07	2.12 ± 0.27**	1.21 ± 0.08††
LVFS, %	49.3 ± 4.6	57.4 ± 2.3	30.8 ± 2.9**	47.6 ± 3.2†††
HR, bpm	633.2 ± 29.4	666.2 ± 16.3	630.0 ± 15.8	663.8 ± 10.4

Parameters at 4-week	AAV9-CTRL +sham (n = 7)	AAV9-NMT2 +sham (n = 6)	AAV9-CTRL +TAC (n = 6)	AAV9-NMT2 +TAC (n = 5)
IVSd, mm	0.96 ± 0.03	0.89 ± 0.03	1.23 ± 0.03***	1.01 ± 0.05††
LVPWd, mm	1.02 ± 0.04	1.03 ± 0.04	1.30 ± 0.04**	1.07 ± 0.08†
LV mass, mg	75.5 ± 3.7	74.5 ± 2.3	160.3 ± 16.8***	85.2 ± 2.0†††
LVIDd, mm	2.47 ± 0.09	2.53 ± 0.08	3.15 ± 0.25*	2.53 ± 0.09†
LVIDs, mm	1.05 ± 0.05	1.04 ± 0.06	2.32 ± 0.26***	1.26 ± 0.14†††
LVFS, %	57.3 ± 1.3	58.9 ± 2.4	27.4 ± 3.0***	50.8 ± 3.9†††
HR, bpm	668.9 ± 16.7	685.7 ± 13.7	598.9 ± 24.1	655.4 ± 17.5

All data are presented as the mean ± SEM. Pressure overload was induced by constricting the transverse aorta using a 28-gauge blunt needle. $^{*}P < 0.05$, $^{**}P < 0.01$, and $^{***}P < 0.001$ vs. sham-operated AAV9-CTRL-injected mice. $^{†}P < 0.05$, $^{††}P < 0.01$, and $^{†††}P < 0.001$ vs. TAC-operated AAV9-CTRL-injected mice. Statistical test was performed by one-way ANOVA with Tukey's post hoc analysis. IVSd, diastolic interventricular septum wall thickness; LVPWd, diastolic left ventricular posterior wall thickness; LV, left ventricular; LVIDd, end-diastolic left ventricular internal dimension; LVIDs, end-systolic left ventricular internal dimension; LVFS, left ventricular fractional shortening; HR, heart rate: PG, pressure gradient.

Supplemental Methods

Animal model of pressure overload by transverse aortic constriction (TAC)

Male mice with a C57BL/6 J background at 7 weeks old (Japan SLC) were subjected to TAC or sham surgeries as previously reported.[1] Briefly, the mice were given intraperitoneal injections of 0.3 mg/kg of medetomidine, 4.0 mg/kg of midazolam, and 5.0 mg/kg of butorphanol. A trans-sternal thoracotomy was performed after deep anesthesia was confirmed, and the aorta was constricted at the arch between the brachiocephalic artery and left common carotid artery by tying a 7.0 suture with a 27- or 28-gauge blunt needle as indicated.[1, 2] The aorta was left with a calibrated stenosis after the needle was removed. The same procedure except for the aorta ligation was carried out on sham-operated mice. The chest was closed, and the animals were allowed to recover.

Western blot analysis

Proteins were extracted from cultured cells or from mouse left ventricles that were homogenized with TissueLyser II (QIAGEN) in lysis buffer (Cell Lysis Buffer, Cell Signaling Technology) containing a protease inhibitor cocktail (BD Biosciences). Protein concentration was determined using a Pierce BCA Protein Assay (Thermo Fisher Scientific). Aliquots of proteins were subjected to SDS-polyacrylamide gel electrophoresis, transferred onto polyvinylidene difluoride membranes (Merck Millipore) or nitrocellulose membranes (Amersham), and probed with the following primary antibodies; NMT1 (1:1000, 11546, Proteintech), NMT2 (1:1000, 412532, Biorbyt), FLAG-tag (1:1000, 14793, Cell Signaling Technology), HA-tag (1:1000, M132-3, MBL life science), MARCKS (1:1000, 10004, 20661, Proteintech), AKT (1:1000, 9272, Cell

Signaling Technology), Phospho-AKT (1:1000, 9271, Cell Signaling Technology), Histone H3 (1:1000, 9715, Cell Signaling Technology), Acetyl-Histone H3 (1:1000, 9649, Cell Signaling Technology), HDAC4 (1:1000, 7628, Cell Signaling Technology), Phospho-HDAC4/HDAC5/HDAC7 (1:1000, 3443, Cell Signaling Technology), Phospho-HDAC4 (1:1000, ab39408, Abcam), CaMKII (1:1000, 4436, Cell Signaling Technology), Phospho-CaMKII (1:1000, 12716, Cell Signaling Technology), Na, K-ATPase (1:1000, ab283318, Abcam), and GAPDH (1:1000, 60004-1-Ig, Proteintech) followed by the appropriate IRDye 680 or IRDye 800 secondary antibodies (1:20000, 925-68070, 925-68071, 925-32210, 925-32210, LI-COR Biosciences). Fluorescent immunoreactive bands were detected by an Odyssey CLX imaging system (LI-COR Biosciences). Optical densities of individual bands were analyzed using ImageJ software (National Institutes of Health) or Image Studio software (LI-COR Biosciences).

Histological analysis for murine hearts

Murine heart samples were fixed in 4% paraformaldehyde solution for paraffin embedding or frozen heart tissues were embedded in the O.C.T. compound (Tissue-Tek). For immunohistochemical staining, the paraffin-embedded tissue sections were incubated with the primary antibody of NMT1 (1:100, 11546, Proteintech) or NMT2 (1:100, 412532, Biorbyt) followed by anti-rabbit IgG antibody labeled with peroxidase (414341, Nichirei Bioscience) with DAB peroxidase substrate system (347-00904, Dojin Co., Ltd.) and counterstained with hematoxylin. Images were acquired using a microscope (BZ-X700, Keyence Co.) using Keyence BZ II Viewer software (Keyence Co.). More than 300 cells from 10 random fields were analyzed for quantification. For assessment of myocardial fibrosis, the paraffin-embedded sections were stained with Elastica-Masson (EM) and

fibrosis fraction were measured using ImageJ software (National Institutes of Health). For assessment of cross-sectional area of cardiomyocytes, the sections were incubated with wheat germ agglutinin (Alexa Fluor 488 conjugated, Thermo Fisher Scientific) and mounted with DAPI-containing mounting media. Cardiomyocyte cross-sectional area was measured by using ImageJ software (National Institutes of Health) from more than 100 cardiomyocytes. For fluorescent immunohistochemical staining, the sections were incubated with the primary antibody of FLAG-tag (1:100, 14793, Cell Signaling Technology) with the secondary antibody of Alexa Fluor 594 (1:1000, R37119, A-21211, Thermo Fisher Scientific) followed with wheat germ agglutinin (Alexa Fluor 488 conjugated, Thermo Fisher Scientific), and then mounted with DAPI-containing mounting media. O.C.T.-embedded sections were incubated with the primary antibody of CD45 (1:100, sc-53665, Santa Cruz Biotechnology Inc.), CD68 (1:800, ab125212, Abcam), or CD45R (1:100, 103201, BioLegend) followed by anti-rat (414311, Nichirei Bioscience) or rabbit IgG antibody labeled with peroxidase with DAB peroxidase substrate system and counterstained with hematoxylin. All images were acquired by a microscope (BZ-X700, Keyence Co.) using Keyence BZ II Viewer software (Keyence Co.).

Patient subjects and immunohistochemical study

We enrolled patients with symptomatic stage C/D heart failure (n=12) and age-matched and sex-matched non-heart failure participants (n=6), all of whom underwent endomyocardial biopsy at Fukushima Medical University Hospital between January 2016 and November 2020. The etiology of the heart failure in the patient group was idiopathic dilated cardiomyopathy. The non-failing heart controls were clinically suspected of

having some cardiac disease based on laboratory testing, electrocardiography, and echocardiography but no specific diagnosis was made according to examinations including endomyocardial biopsy findings and coronary angiography. Heart failure and idiopathic dilated cardiomyopathy were diagnosed by independent board-certified cardiologists according to the guidelines.[3] We excluded patients who had a previous history of myocardial infarction or coronary revascularization, a known primary cardiomyopathy condition, or any systemic disease that is known to be associated with the development of cardiomyopathy. The ventricular tissues were obtained from the right ventricular side of the interventricular septum. Clinical data including echocardiography, laboratory tests and hemodynamic assessment by right heart catheterization were obtained with our standard methods.[4, 5] Immunohistochemistry was performed on paraffin-embedded biopsy specimens, and 3-μm sections were cut from paraffin blocks and placed onto slides. After deparaffinization and rehydration, the sections were stained with incubated with the primary antibody of NMT1 (1:100, 11546, Proteintech) or NMT2 (1:100, 412532, Biorbyt), followed by horseradish peroxidase-conjugated secondary antibody (424151, Nichirei Bioscience) with DAB peroxidase substrate system (347-00904, Dojin Co., Ltd.) and counterstained with hematoxylin. For fluorescent immunohistochemical analysis, the sections were incubated with anti-MARCKS antibody (1:100, 10004, Proteintech) followed by the secondary antibody of Alexa Fluor 647 (1:1000, ab150159, Abcam) and wheat germ agglutinin, and then mounted with DAPI-containing mounting media. Images were acquired using a microscope (BZ-X700, Keyence Co.) using Keyence BZ II Viewer software. More than 300 cells from 10 random fields were analyzed for quantification.

Adeno-associated virus 9 (AAV9) construction and vector delivery in mice

To prepare AAV9 to knockdown NMT2 in the heart, a short-hairpin RNA (shRNA) targeted to mouse *Nmt2* (NM_008708.2) was prepared[6] using the following oligonucleotides: Target 1, sense, 5'-GGATGGTAGAAATCAACTTTC-3'; Target 1, antisense, 5'-GAAAGTTGATTTCTACCATCC-3'; Target 2, sense, 5'-GCGCTCATTATAGCCAAATTG-3'; Target 2, antisense, 5'-CAATTTGGCTATAATGAGCGC-3'. These oligonucleotides were annealed and cloned into Xba I and Spe I or Sal I and Xho I sites in pAAV-2xU6 vector (Takara Bio). A shRNA directed against LacZ (NM_009752.2), was also generated by cloning into pAAV-2xU6 vector as a control, with the following oligonucleotides: Target 1, sense, 5'-GGGCCAACGTGAACTTGTACA-3'; Target 1, antisense: 5'-TGTACAAGTTCACGTTGGCCC-3'; Target 2, sense, 5'-GGCTGCTGAAGATGAAGATGG-3'; Target 2, antisense, 5'-CCATCTTCATCTTCAGCAGCC-3'. For preparation for AAV9 to overexpress NMT2 in the heart,[6] pAAV-CMV vector (Takara Bio) was constructed by subcloning mouse *Nmt2* (NM_008708.2) with an N-terminal FLAG tag (epitope tag, amino acid sequence DYKDDDDK) at the EcoR I and Sal I sites. A pAAV-CMV-LacZ (Addgene plasmid #105531) was used as a control. To create recombinant AAV9, HEK293T cells were transfected with the pAAV-2xU6 vector encoding shRNA target to NMT2 or LacZ or pAAV-CMV vector encoding NMT2 or LacZ, along with a pHelper vector (Takara Bio) and pAAV2/9n (Addgene plasmid #112865) using TransIT-293 Reagent (Mirus Bio). Seventy-two hours after transfection, cells were harvested and the collected AAV9 was purified using AAVpro Purification Kit (TaKaRa) and viral titer was calculated using AAV Titration Kit (TaKaRa). To administer recombinant AAV9, wild-type male mice

with a C57BL/6J background (Japan SLC) aged at six weeks (body weight range, 20-23 g) were injected via lateral tail vein with 100 μL of AAV9 solution with 10^{11} genome-containing units per mouse. One week after AAV9 injection, the mice were subjected to TAC or sham surgery.

Echocardiography

Transthoracic echocardiography was performed using Vevo 2100 High-Resolution Imaging System (Visual Sonics Inc.) with a 20- or 40- MHz imaging transducer.[1] M-mode images of the parasternal short-axis view at papillary muscle level were captured on conscious mice and all parameters were averaged over at least 4 cardiac cycles for analysis. Left ventricular (LV) fractional shortening and LV mass were calculated as 100 × [end-diastolic LV internal dimension (LVIDd) – end-systolic LV internal dimension (LVIDs)]/LVIDd and 1.05 × {[LVIDd + diastolic interventricular septum wall thickness (IVSd) + diastolic LV posterior wall thickness (LVPWd)]^3-(LVIDd)^3}, respectively. The peak pressure gradient was measured using pulsed-wave Doppler at the aortic arch on the mice lightly anesthetized by titrating isoflurane (0.5–1.5%) to achieve a heart rate of around 400/min.

Reverse transcription-quantitative polymerase chain reaction (RT-qPCR)

Total RNA was extracted from cultured cells or mouse hearts using Trizol reagent (Thermo Fisher Scientific) according to the manufacturer's protocol. cDNA was synthesized using ReverTra Ace qPCR RT Master Mix (Toyobo Co., Ltd.). Quantitative PCR was performed to determine the mRNA expression of *Nppa*, *Nppb*, *Myh7*, *Col1a1*, *Col8a1*, *Il1b*, *Ifng* and *Actb* using THUNDERBIRD SYBR qPCR Mix (Toyobo Co., Ltd.)

in a CFX Connect real-time PCR System (Bio-Rad) with Bio-Rad CFX Manager 3.1 software (Bio-Rad). A delta CT method was used for the cell samples and a standard curve method on serially diluted templates was applied for the heart samples. All data were normalized to *Actb* and expressed as a fold increase of the control group. Primer sequences are described in the following Table.

Primers used for RT-qPCR

	Gene			Sequence	
Mouse	*Nppa*	Forward	5'-	TCGTCTTGGCCTTTTGGCT	-3'
		Reverse	5'-	TCCAGGTGGTCTAGCAGGTTCT	-3'
	Nppb	Forward	5'-	AAGTCCTAGCCAGTCTCCAGA	-3'
		Reverse	5'-	GAGCTGTCTCTGGGCCATTTC	-3'
	Myh7	Forward	5'-	ATGTGCCGGACCTTGGAAG	-3'
		Reverse	5'-	CCTCGGGTTAGCTGAGAGATCA	-3'
	Col1a1	Forward	5'-	CCTGGCAAAGACGGACTCAAC	-3'
		Reverse	5'-	GCTGAAGTCATAACCGCCACTG	-3'
	Col8a1	Forward	5'-	CGGGAGTAGGAAAACCAGGAGTG	-3'
		Reverse	5'-	CTCGGCCCAAGAACCCCAGGAA	-3'
	Il1b	Forward	5'-	TGAAGTTGACGGACCCCAAA	-3'
		Reverse	5'-	TGATGTGCTGCTGTGAGATT	-3'
	Ifng	Forward	5'-	CGGCACAGTCATTGAAAGCCTA	-3'
		Reverse	5'-	GTTGCTGATGGCCTGATTGTC	-3'
	Actb	Forward	5'-	CTGTCCCTGTATGCCTCTG	-3'
		Reverse	5'-	ATGTCACGCACGATTTCC	-3'
Rat	*Nppa*	Forward	5'-	CTGATGGATTTCAAGAACCTGCT	-3'
		Reverse	5'-	GAGAGAGGGAGCTAAGTGCC	-3'
	Nppb	Forward	5'-	GTGCTGCCCCAGATGATTCT	-3'
		Reverse	5'-	CTCCAGCAGCTTCTGCATCG	-3'
	Myh7	Forward	5'-	CTGGCACCGTGGACTACAAT	-3'
		Reverse	5'-	GCCCTTGTCTACAGGTGCAT	-3'
	Actb	Forward	5'-	GCCTTCCTTCCTGGGTATGG	-3'
		Reverse	5'-	AATGCCTGGGTACATGGTGG	-3'

Immunofluorescence and assessment of myocyte surface area in cultured myocytes

For immunofluorescence analysis, the adhered cells were fixed by 4% paraformaldehyde at 37°C for 15 min, and permeabilized with 1% Triton X-100 for 15 min, and blocked

with 2% normal bovine serum (Sigma) for 1 h at room temperature, and then incubated with specific primary antibodies as follows; Na, K-ATPase (1:100, 3010, Cell Signaling Technology) and HA-tag (1:100, M132-3, MBL life science). Those were followed by incubation with the appropriate secondary antibodies, including Alexa Fluor 488 (1:1000, ab150105, Abcam), Alexa Fluor 594 (1:1000, R37119, A- 21211; Thermo Fisher Scientific), and Alexa Fluor 647 (1:1000, ab150159, Abcam), or Phalloidin-iFluor 488 Reagent (1:1000, ab176753, Abcam), and then mounted with DAPI-containing mounting media (Fluoro Gel II, Electron Microscopy Sciences). For assessment of cardiac myocyte surface area, the fixed cells were stained with Phalloidin-iFluor 488 Reagent and then mounted with DAPI-containing mounting media. The cell surface areas were determined by using ImageJ software (National Institutes of Health) from more than 100 cells from at least five different fields of each culture. All images were acquired by a microscope (BZ-X700, Keyence Co.) using Keyence BZ II Viewer software (Keyence Co.).

Cell culture and isolation of neonatal rat cardiomyocytes (NRCM)

H9c2 rat embryonic cardiac myoblasts were purchased from ATCC (CRL-1446). The cells were cultured in Dulbecco's modified Eagle's medium (DMEM, Sigma) supplemented with 10% fetal bovine serum, 100 μg/mL of streptomycin, and 100 IU/mL of penicillin at 37 °C in the presence of 5% CO_2. NRCM was isolated from hearts of 1- to 2-day-old Sprague-Dawley rats as previously reported[1] with enzymatic dissociation by collagenase type II (Worthington), and were cultured in DMEM (Sigma) containing 20% fetal bovine serum, 10% penicillin-streptomycin-glutamine, and 100 mM BrdU (Sigma) for 24 h. The media were changed into serum-free DMEM containing 10% penicillin-streptomycin-glutamine, 100 mM BrdU (Sigma), 1 μg/mL insulin (Sigma), and 5 μg/mL

transferrin (Sigma), and cells were incubated for an additional 24 h, and then used for the experiments.

Adenovirus construction and infection

Target-specific shRNA against rat *Nmt2* mRNA (NM_008708.2, sense: 5'-GCACATCATTGACACCTTTGT-3') was designed by using BLOCK-iT RNAi Designer (Thermo Fisher Scientific). A recombinant adenoviral vector expressing shRNA was constructed with BLOCK-iT U6 RNAi Entry Vector Kit and BLOCK-iT Adenoviral RNAi Expression System (Thermo Fisher Scientific) according to the manufacturer's instructions. The adenovirus was amplified in HEK293A cells and purified using a freeze-thaw cycle. The virus titer was determined by QuickTiter Adenovirus Titer Immunoassay Kit (Cell Biolabs). NRCM was infected with an adenoviral vector expressing shRNA targeted to NMT2 (Ad5-shNMT2) at a multiplicity of infection of 100. LacZ was used as a control (Ad5-shCTRL).

Transfection with small interfering RNA (siRNA) and plasmid DNA

H9c2 cells were transfected with scrambled negative control siRNA (37007, Santa Cruz Biotechnology), NMT1-specific siRNA (s141349, 4390771, Thermo Fisher Scientific), or NMT2-specific siRNA (s145595, 4390851, Thermo Fisher Scientific) using ScreenFect A (Wako) according to manufacturer's instructions. For plasmid DNA transfection, H9c2 myocytes were transfected using ScreenFect A (Wako) according to the manufacturer's instructions.

Click chemistry for labeling N-myristoylated proteins

For click metabolic labeling,[7, 8] Click-iT myristic acid azide (Thermo Fisher Scientific) at the concentrations of 50 μM was introduced to the cell culture of H9c2 cells with 2% fatty acid-free bovine serum albumin (Sigma) instead of DMEM or NRCM with a standard medium, and cells were incubated for 24 h. Cells without adding the myristic acid azide were set for a negative control for the validation. Cells were lysed with the urea lysis buffer which consists of 8 M urea, 200 mM Tris HCl pH 8, 4% CHAPS, 1 M NaCl, and protein concentration was determined using a Pierce BCA Protein Assay (Thermo Fisher Scientific). For a click reaction, 80 μg of protein was incubated with alkyne-agarose resin with 50% slurry by Click-iT protein enrichment technology (Click-iT Protein Enrichment Kit, Thermo Fisher Scientific) for 18 h on a rotator at room temperature. Following centrifugation, the beads were transferred to a fritted column and subjected to stringent washing with the buffer containing 8 M urea, 1% SDS, 20% acetonitrile at 3 times, and were reduced with 10 mM DTT, and then alkylated by 20 mM iodoacetamide. Subsequently, the beads were incubated with modified porcine trypsin (Promega) and incubated overnight at 37°C. After centrifugation, the supernatant containing the digested peptides was transferred and resuspended in 2% acetonitrile and 0.1% TFA for subsequent analysis by liquid chromatography-tandem mass spectrometry (LC-MS/MS).

Liquid chromatography-tandem mass spectrometry analysis

The LC-MS/MS was performed using an Easy-nLC1000 system (Thermo Fisher Scientific) coupled to a Q Exactive mass spectrometer 1000 (Thermo Fisher Scientific). The digested peptide samples were loaded into a pre-column of an Acclaim PepMap 100 C18 LC column with 75 μm × 20 mm inner diameter (Thermo Fisher Scientific). For the separation of the peptides, a multistep linear gradient elution was applied using reverse-

phase liquid chromatography (RPLC) mobile phase A of 0.1% formic acid in water and RPLC mobile phase B of 0.1% formic acid in acetonitrile with an Easy-spray PepMap C18 column with 75 μm × 15 mm inner diameter (Thermo Fisher Scientific). The gradient elution method using the EASY-nLC 1000 system at flow rates of 200 nL/min was carried out as the following program: 0% solvent B for 1 min, an increase from 0% to 5% solvent B for 4 min, from 5% to 35% solvent B for 20 min, and from 35% to 100% solvent B for 5 min. The full survey scan was operated in data-dependent mode at a resolution of 60,000 in the range of 350-1800 m/z by the Q Exactive mass spectrometer 1000. Up to 10 of the most abundant isotope patterns with charge +2 or higher from the survey scans were selected with an isolation window of 2.0 m/z and fragmented by higher-energy collision dissociation (HCD) with normalized collision energies of 25. The maximum ion injection times for the survey and MS/MS scans acquired with a resolution of 30,000 at 400 m/z were 10 and 50 ms, respectively. An ion target value for MS was set to 10^6, MS/MS to 10^5, and the intensity threshold was set to 1.8×10^3.

Proteomics data analysis

All raw data acquired from LC-MS/MS spectra were processed with Proteome Discoverer version 1.4 (Thermo Fisher Scientific). The amino acid sequences of the peptides were identified using MASCOT (MASCOT free version, Matrix Science) and Sequest-HT (Thermo Fisher Scientific) search engines against Rat database in the SwissProt and Uniprot (downloaded on April 2021). The cleavage enzyme, trypsin (full cleavage), was specified to accommodate up to two missing cleavages. The tolerance of precursor ions and fragment ions was set to 10 ppm and 0.02 Da, respectively. The range was set between the minimum precursor mass of 350 Da and the maximum precursor mass of 5000 Da.

Scaffold 5 (Proteome Software, Inc) was used to report MS/MS-based peptide and protein identifications and intensity-based label-free quantification based on precursor ion intensity by parallel reaction monitoring. The peptide and protein threshold for the certainty of a peptide identification were set at more than 95% by the Peptide Prophet algorithm.[9] The label-free quantification of LC-MS/MS was applied to determine protein abundance in each sample by measuring the intensity of the corresponding MS spectrum features of the protein.[10] Data were exported from Scaffold for statistical analysis of the differences in mean intensities among multiple replicate samples. Differential abundance was concluded when the p-value of the comparison was below a predefined cutoff of 0.05.

Construction of DNA plasmid

Rat *Marcks* (NM_008538.2) cDNA was obtained by reverse transcription-polymerase chain reaction using total RNA from rat H9c2 cells. *Marcks* was amplified with the forward primer 5'-AAAAAGCTTCATGGGTGCCCAGTTCTCC-3' and reverse primer 5'-AAAGGATCCTTACTCGGCCGTTGGCGC-3'. The fragment was inserted into CMV-driven expression vector with an N-terminal double HA tag (pHAHA, Addgene plasmid #12517) at Hind III and BamH I sites. Mutant *Marcks* with replacement of N-terminal glycine to alanine was designed based on wild-type *Marcks* by mutagenesis using PrimeSTAR Mutagenesis Basal Kit (Takara Bio) with the forward primer, 5'-TTCATGGCTGCCCAGTTCTCCAAGACC-3' and reverse primer, 5'-CTGGGCAGCCATGAAGCTTGCGTAATC-3'. Mouse *Nmt2* (NM_008708.2) cDNA was obtained from RNA from C57BL/6J mouse heart. *Nmt2* as amplified by PCR with the forward primer 5'-AAAGAATTCATGGCGGAGGACAGC-3' and reverse primer 5'-AAAGTCGACCTACTGTAGAACAAGTCC-3'. The fragment was inserted into

pAAV-CMV vector (Takara Bio) at EcoR I and Sal I sites. The obtained fragment was directly subcloned into the plasmid constructs were verified by restriction digestion and DNA sequencing.

Cell viability assay

H9c2 cells were seeded at 0.8×10^4/well in 96-well plates and transfected with siRNA. The number of viable cells were analyzed using a MTT assay (Promega). The data were expressed as a relative ratio to the control.

Ca^{2+}/calmodulin-dependent protein kinase II (CaMKII) activity assay

CaMKII activity of H9c2 myocytes was analyzed using CycLex CaM kinase II Assay Kit (MBL life science) according to the manufacturer's instructions. The proteins (10 μg) measured by BCA Protein Assay obtained from the cell lysates were loaded onto microliter wells coated with Syntide-2, a specific substrate to CaMKII, and with kinase reaction buffer with or without Ca^{2+}/calmodulin. CaMKII activity was quantitatively evaluated by measuring absorbance using a spectrophotometric plate reader at dual wavelengths of 450/540 nm based on a constructed standard curve using active CaMKII (MBL life science). The data were expressed as a relative ratio to the control.

Pharmacological inhibition of CaMKII

CaMKII inhibitor (KN-93, ab120980, Abcam, 5 μM) was administered to the H9c2 myocytes 1 h prior to Ang II stimulation.

Subcellular fractionations of the murine hearts

Subcellular fractionations of the heart tissue sample were performed using the subcellular protein fractionation kit for tissues (87790, Thermo Fisher Scientific) as per the instructions provided by the manufacturer. In brief, 50 mg of heart tissue was initially homogenized by using a glass-Teflon homogenizer with cytoplasmic extraction buffer, and then centrifuged the tissue at 500 g for 5 min. The supernatant was collected and considered as a cytoplasmic fraction. The pellet was dissolved in membrane extraction buffer and centrifuged at 3,000 g for 5 min. The supernatant was collected as a membrane fraction.

RNA sequencing

Total RNA isolated from the heart tissues using Trizol reagent (Thermo Fisher Scientific)[11] was purified with a DNA-free DNA Removal Kit (Thermo Fisher Scientific). Concentrations of the total RNA were measured using NanoDrop 2000/2000c Spectrophotometers (Thermo Fisher Scientific), and RNA integrity of equal amounts of total RNA (1 μg) were assessed by Agilent 2100 Bioanalyzer (Agilent Technologies) with Agilent RNA6000 nano Reagent at Beijing Genomic Institute. cDNA libraries made from RNA samples were prepared and were sequenced using BGISEQ-500 (Beijing Genomics Institution) to generate 150 bp paired-end raw reads. The Low-quality reads were filtered, and the clean reads were aligned to the reference genome (GCF_000001635.26_GRCm38.p6) using HISAT. Gene expression was computed based on the reads, and differentially expressed genes and gene ontology analyses were analyzed on Dr. Tom platform software (Beijing Genomic Institute). Statistical significance was based on a Q-value below 0.05.

Statistical analysis

The Shapiro-Wilk test was conducted to assess whether the data followed a normal distribution. Parametric data were expressed as the mean ± standard error of the mean (SEM), while nonparametric data were expressed as the number (%) or median (25th - 75th percentiles). For comparisons between two groups, the unpaired Student's t-test was conducted for parametric data, and the Mann-Whitney U-test was used for nonparametric data. Fisher’s exact test was employed to compare categorical variables. One-way analysis of variance (ANOVA) followed by Tukey's post-hoc test for multiple pairwise comparisons was applied when more than two groups were evaluated. Survival time was analyzed using Kaplan-Meier methods with the log-rank test used to compare groups. Data were analyzed using Statistical Package for Social Sciences version 28.0 (SPSS Inc) and GraphPad Prism version 9.5.1 (GraphPad Software).

Ethical statement

All animal studies were reviewed and approved by the Fukushima Medical University Animal Research Committee (approval number, 2021129). The protocols complied with relevant ethical regulations. All experiments were performed following the guidelines in the Guide for the Use and Care of Laboratory Animals from the Institute for Laboratory Animal Research. All efforts were made to minimize the suffering of the animals. The protocols involving human participants were approved by the institutional ethics committee of Fukushima Medical University Hospital (approval number, 2020-309). The investigation conforms with the principles outlined in the Declaration of Helsinki.

Supplementary References

1. Misaka T, Murakawa T, Nishida K, et al. FKBP8 protects the heart from hemodynamic stress by preventing the accumulation of misfolded proteins and endoplasmic reticulum-associated apoptosis in mice. *J Mol Cell Cardiol*. 2018;114:93-104.
2. Souders CA, Borg TK, Banerjee I and Baudino TA. Pressure overload induces early morphological changes in the heart. *Am J Pathol*. 2012;181(4):1226-35.
3. Ponikowski P, Voors AA, Anker SD, et al. 2016 ESC Guidelines for the diagnosis and treatment of acute and chronic heart failure: The Task Force for the diagnosis and treatment of acute and chronic heart failure of the European Society of Cardiology (ESC). Developed with the special contribution of the Heart Failure Association (HFA) of the ESC. *Eur J Heart Fail*. 2016;18(8):891-975.
4. Misaka T, Yoshihisa A, Yokokawa T, et al. Plasma levels of melatonin in dilated cardiomyopathy. *J Pineal Res*. 2019;66(4):e12564.
5. Wada K, Misaka T, Yokokawa T, et al. Blood-Based Epigenetic Markers of FKBP5 Gene Methylation in Patients With Dilated Cardiomyopathy. *J Am Heart Assoc*. 2021;10(21):e021101.
6. Doroudgar S, Volkers M, Thuerauf DJ, et al. Hrd1 and ER-Associated Protein Degradation, ERAD, are Critical Elements of the Adaptive ER Stress Response in Cardiac Myocytes. *Circ Res*. 2015;117(6):536-46.
7. Agard NJ, Prescher JA and Bertozzi CR. A strain-promoted [3 + 2] azide-alkyne cycloaddition for covalent modification of biomolecules in living systems. *J Am Chem Soc*. 2004;126(46):15046-7.

8. Thirumurugan P, Matosiuk D and Jozwiak K. Click chemistry for drug development and diverse chemical-biology applications. *Chem Rev*. 2013;113(7):4905-79.
9. Keller A, Nesvizhskii AI, Kolker E and Aebersold R. Empirical statistical model to estimate the accuracy of peptide identifications made by MS/MS and database search. *Anal Chem*. 2002;74(20):5383-92.
10. Al Shweiki MR, Monchgesang S, Majovsky P, et al. Assessment of Label-Free Quantification in Discovery Proteomics and Impact of Technological Factors and Natural Variability of Protein Abundance. *J Proteome Res*. 2017;16(4):1410-1424.
11. Kimishima Y, Misaka T, Yokokawa T, et al. Clonal hematopoiesis with JAK2V617F promotes pulmonary hypertension with ALK1 upregulation in lung neutrophils. *Nat Commun*. 2021;12(1):6177.

Data Availability

The LC-MS/MS data underlying this article are available in its online supplementary material. The RNA sequencing data generated in this study have been deposited in the DNA Data Bank of Japan database under accession code DDBJ PRJDB14076.